Data Quality Control of Ka-band Cloud Radar for Detecting Cumulus Clouds

Takeshi Maesaka, Koyuru Iwanami, Shin-ichi Suzuki, Yukari Shusse, and Namiko Sakurai
National Research Institute for Earth Science and Disaster Resilience, Tsukuba, JAPAN

NIED

Summary

Ka-band cloud radar network was deployed around Tokyo metropolitan area to detect cumulus clouds which are developing to sever cumulonimbus. For the early detection of these clouds, the radars must have a high-sensitivity. But the high-sensitivity causes some new problems that we have never concerned. In this paper, we present a data quality control procedure for detecting cumulus clouds which are developing to cumulonimbus. The methods presented in ths poster are applied to the observed radar data, and show good performance for the cumulus detection.

Radar and Specifications

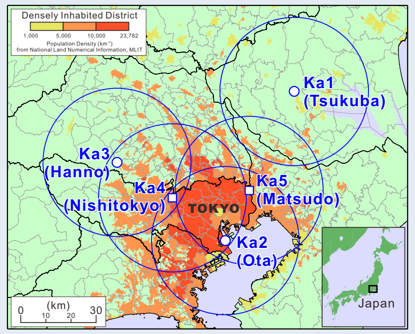

Figure 1. Distributions of five Ka-band cloud radars (top) and their photos (bottom). Blue circles indicate the observation ranges (r=30 km) of each radar. Colored areas indicate a densely inhabited districts. The radars indicated by open circles are dual-polarization radars (transmission: simultaneous H/V or single polarization, dual-receiver), while open squares indicate single polarization (H) radars.

Table 1. Specifications of cloud radar.

Features	Specifications
Frequency	34.815 GHz - 34.905 Ghz (Ka-band)
Occupied bandwidth	13 MHz
Microwave amplifier	Extended Interaction Klystron (EIK)
Transmit power	3 kW
Pulse compression	Linear frequency modulation (2 MHz)
Pulse width (short)	0.5 μs and 1.0 μs
Pulse width (long)	30 μs, 45 μs, 55 μs, 80 μs and 100 μs
Pulse repetition frequency	Max. 2500 Hz @ τ=30 μs
IF digitizer	16 bit, 36 MHZ
Antenna	Cassegrain antenna (⌀=2.2 m)
Antenna gain	54 dB (Typ.)
Beam width	0.3 deg (Typ.)
Antenna Sidelobe level	-23 dB (Typ.)
Polarization	H/V simultaneous or single H or V
Observation range	30 km
Output data resolution	75 m or 150 m
Nyquist Velocity	5.38 ms^{-1} @ PRF=2500 Hz
Dual PRF	3:2, 4:3 and 5:4 for velocity de-aliasing
Clutter Filters	IIR or spectrum interpolation
Output Data	Pr, Z, V, W, SQI, SNR and I/Q
Output Data (Simul. dual-pol.)	Z_{DR}, ρ_{HV}, Φ_{DP} and K_{DP}
Output Data (Single, dual-receive)	$LDR_{H\ or\ V}$, $\rho_{H\ or\ V}$, $\Phi_{H\ or\ V}$

Weak Echo Detection

The reflectivity of early stage cumulus cloud is mostly the same as the noise level (-30 dBZ — -20 dBZ) of our Ka-band radar. So we must detect the cloud signal from the noise. For detecting the cloud echo, a moving average of the received power with a window size of 5 rays and 5 range bins is calculated. The range bin and beam widths of our radar are 150 m and 0.3 degrees. This calculation deletes the noise variance to retrieve the cloud echo whose horizontal scale is larger than 750 m.

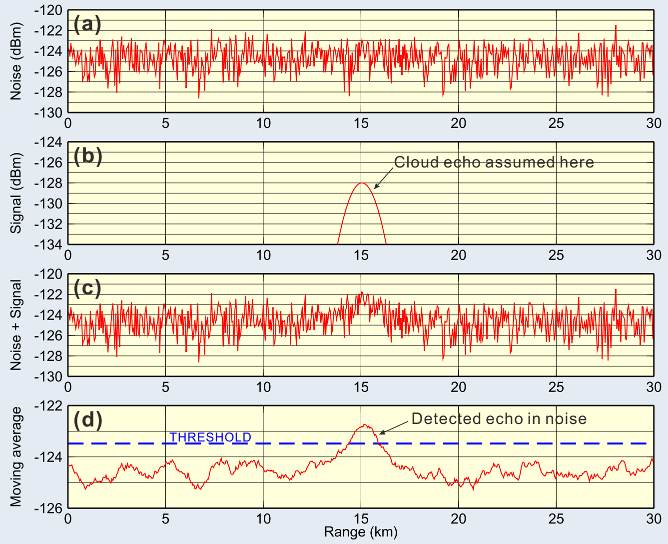

Figure 2. Conceptual range-profiles of received power for explaining the weak echo detection by moving average. a) Noise, b) Signal (cloud echo), c) Composition of noise and signal (supposed to be observed), and d) Moving average of profile (c).

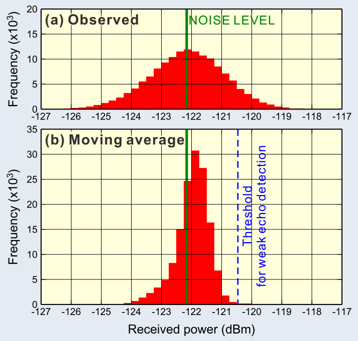

Figure 3. Histograms of noise power observed by Ka5 radar. a) Observed. b) Moving average (5 rays and 5 range bins).

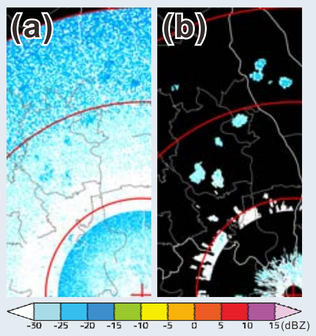

Figure 4. Radar reflectivity PPI observed by Ka5 radar. a) Observed. b) After the weak echo detection.

Range Sidelobe

Pulse compression is used to increase the range resolution as well as the signal to noise ratio. The range sidelobe is not negligible in Ka-band cloud radar, because the reflectivity of our target is -30 dBZ — -10 dBZ. The data contaminated by the sidelobe is deleted by using the predetermined range sidelobe pattern.

GET POSTER VIA QR CODE

Maesaka et.al. 2015: Cloud radar network in Tokyo metropolitan area for early detection of cumulonimbus generation. 37th Conf. on Radar Meteorol. at Norman, Poster 174.
https://ams.confex.com/ams/37RADAR/webprogram/Paper275910.html

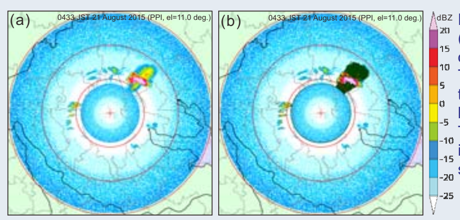

Figure 5. a) Reflectivity PPI (Ka1 radar) including the obvious range sidelobe. b) The same as (a), but with the detected range sidelobe colored by dark green. The details of this method is described in the poster showed above.

Second-Trip Removal

Because of the high sensitivity, our Ka-band cloud radar detects second-trip echo much more than the other band radar. Signal Quality Index (SQI; a.k.a. normalized coherent power) is usually used to remove the second trip echo, but this also deletes the weak echo from early stage cumulus. We use the reflectivity comparison between high and low PRFs to remove the second-trip. Furthermore the second trip echo is simulated from wide area rainfall information observed by operational weather radar. The SQI method is applied only in the simulated area.

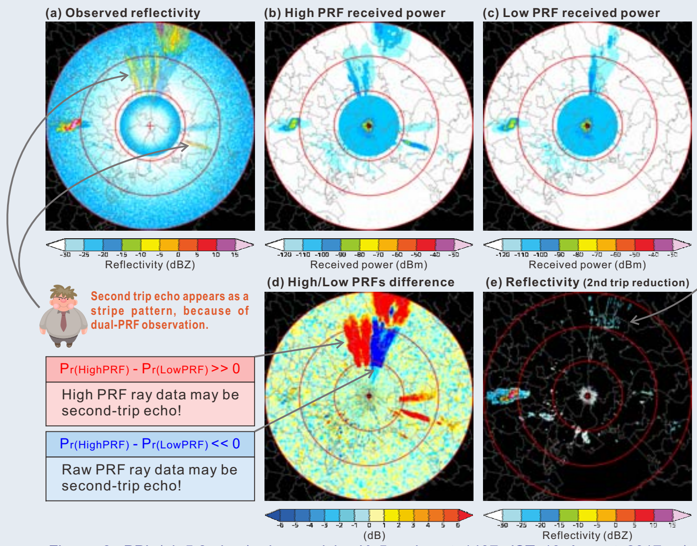

Figure 6. PPI (el=5.8 deg.) observed by Ka5 radar at 1407 JST 19 August 2017. a) Observed reflectivity, b) Moving average (5 rays and 5 range bins) of received power observed by high PRF, c) The same as (b) but for low PRF, d) Received power ratio of high to low PRFs in decibels, and e) Reflectivity from which the second trip echo is removed. Radar range rings are drawn every 10 km.

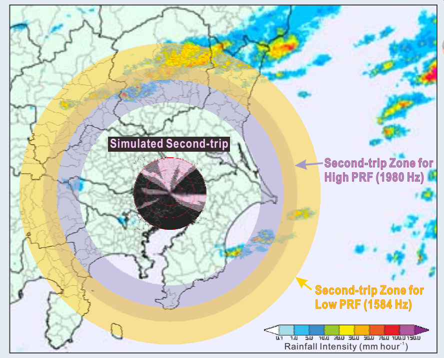

Figure 7. Rainfall map by Japan Meteorological Agency's (JMA's) operational radars at 1405 JST 19 August 2017. Violet and yellow shades indicate the Ka5 radars' second trip zones for high and low PRFs, respectively. The simulated second-trip area is colored with pink in the radar range (black area).

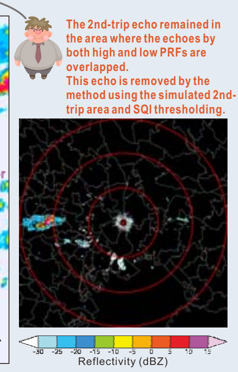

Figure 8. The same as Fig. 6e but the area where SQI is less than 0.5 in the simulated second trip are also removed.

Gas Attenuation Correction

Gas attenuation of Ka-band is not negligible because it is 10 times larger than those of S-, C-, and X-bands. The path-integrated attenuation is calculated from the objective analysis or the numerical simulation data to include the attenuation into radar reflectivity. The calculation is based on Millimeter-wavelength Propagation Model (MPM93, Liebe et al. 1993).

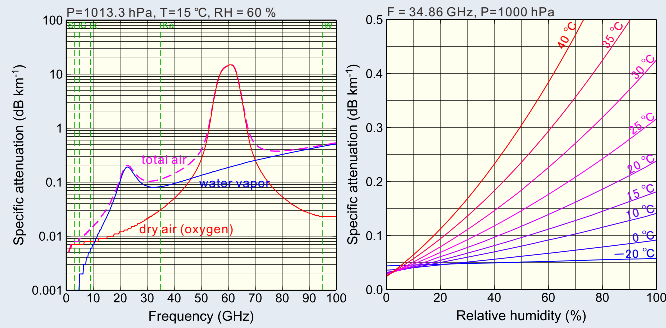

Figure 9. Left) Specific attenuations (dry air, water vapor, and the total) to radio frequency. Right) Specific attenuation of total air to relative humidity.

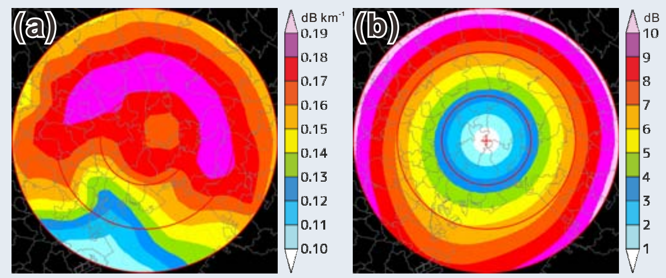

Figure 10. a) Specific and b) 2-way gas attenuations calculated from JMA's Local Forecast Model (LFM, 2 km horizontal resolution). These analyses assume the Ka5 radar (el=2.7 deg.) at 1300 JST 7 July 2017.

Examples

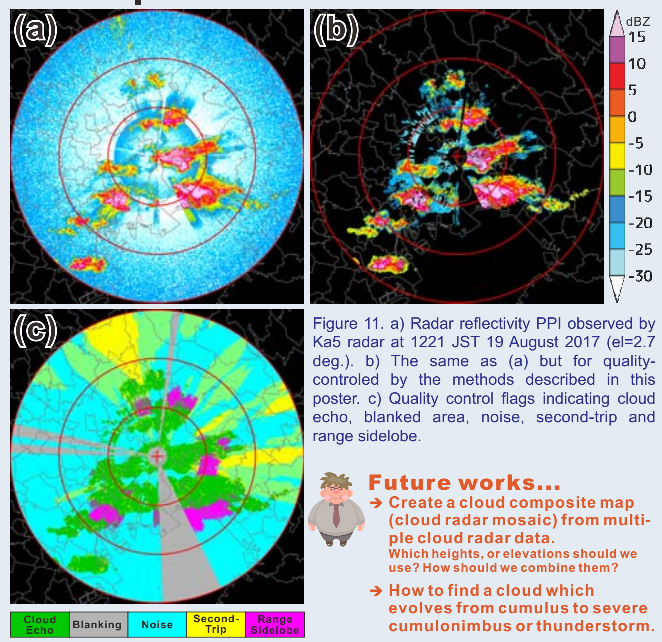

Figure 11. a) Radar reflectivity PPI observed by Ka5 radar at 1221 JST 19 August 2017 (el=2.7 deg.). b) The same as (a) but for quality-controled by the methods described in this poster. c) Quality control flags indicating cloud echo, blanked area, noise, second-trip and range sidelobe.

Future works...

- **Create a cloud composite map (cloud radar mosaic) from multiple cloud radar data.**
  Which heights, or elevations should we use? How should we combine them?
- **How to find a cloud which evolves from cumulus to severe cumulonimbus or thunderstorm.**

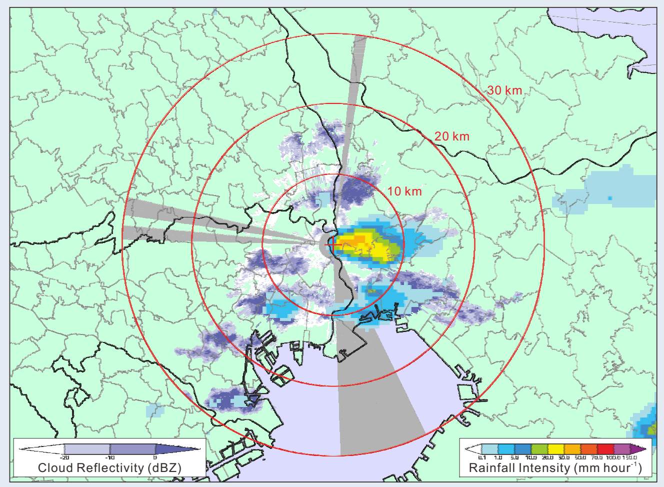

Figure 12. Cloud reflectivity PPI observed by Ka5 radar at 1221 JST 19 August 2017. Rainfall intensity observed by NIED and MLIT X-band dual polarization radars at 1225 JST 19 August 2017 is superimposed on the cloud reflectivity.